

# Pyrimidine-Based Push–Pull Systems with a New Anchoring Amide Group for Dye-Sensitized Solar Cells

Egor V. Verbitskiy <sup>1,2,\*</sup>, Alexander S. Steparuk <sup>1</sup>, Ekaterina F. Zhilina <sup>1</sup>, Viktor V. Emets <sup>3</sup>, Vitaly A. Grinberg <sup>3</sup>, Ekaterina V. Krivogina <sup>4</sup>, Sergey A. Kozyukhin <sup>4,5</sup>, Ekaterina V. Belova <sup>6</sup>, Petr I. Lazarenko <sup>7</sup>, Gennady L. Rusinov <sup>1,2</sup>, Alexey R. Tameev <sup>3</sup>, Jean Michel Nunzi <sup>8,9</sup> and Valery N. Charushin <sup>1,2</sup>

1 I. Postovsky Institute of Organic Synthesis, Ural Branch of the Russian Academy of Sciences, S. Kovalevskaya Str., 22, Ekaterinburg 620108, Russia; steparuk96@mail.ru (A.S.S.); efzhil-ina@ios.uran.ru (E.F.Z.); g.rusinov@mail.ru (G.L.R.); valery-charushin-562@yandex.ru (V.N.C.)

2 Department of Organic and Biomolecular Chemistry, Chemical Engineering Institute, Ural Federal University, Mira St. 19, Ekaterinburg 620002, Russia

3 A. N. Frumkin Institute of Physical Chemistry and Electrochemistry, Russian Academy of Sciences, Moscow 119071, Russia; victoremets@mail.ru (V.V.E.); vitgreen@mail.ru (V.A.G.); altam2001@mail.ru (A.R.T.)

4 N. S. Kurnakov Institute of General and Inorganic Chemistry, Russian Academy of Sciences, 31, Leninsky Pr., Moscow 119991, Russia; ekaterina3141@mail.ru (E.V.K.); sergkoz@igic.ras.ru (S.A.K.)

5 Moscow Institute of Physics and Technology (National Research University), 9 Institutskiy per., Dolgoprudny 141701, Russia

6 Department of Chemistry, Moscow State University, Moscow 119991, Russia; catrine2@mail.ru

7 Institute of Advanced Materials and Technologies, National Research University of Electronic Technology, Moscow, Zelenograd 124498, Russia; lpi@org.miet.ru

8 Nanomaterials Research Institute, Kanazawa University, Kanazawa 920-1192, Japan;

9 Department of Physics, Engineering Physics and Astronomy, Queen's University, Kingston K7L-3N6, ON, Canada; nunzijm@queensu.ca (J.M.N.)

\* Correspondence: verbitskye@yandex.ru

General Information.....	Error! Bookmark not defined.
Fabrication and <i>J</i> – <i>V</i> characterization of DSSCs.....	Error! Bookmark not defined.
Characterization of photoanodes by modulation spectroscopy.....	Error! Bookmark not defined.
Figure S1. <sup>1</sup> H NMR (500 MHz, CDCl <sub>3</sub> ) spectrum of 6.....	Error! Bookmark not defined.
Figure S2. <sup>13</sup> C NMR (126 MHz, CDCl <sub>3</sub> ) spectrum of 6.....	Error! Bookmark not defined.
Figure S3. <sup>1</sup> H NMR (500 MHz, CDCl <sub>3</sub> ) spectrum of 8.....	Error! Bookmark not defined.
Figure S4. <sup>13</sup> C NMR (126 MHz, CDCl <sub>3</sub> ) spectrum of 8.....	6
Figure S5. <sup>1</sup> H NMR (500 MHz, CDCl <sub>3</sub> ) spectrum of 9.....	Error! Bookmark not defined.
Figure S6. <sup>13</sup> C NMR (126 MHz, CDCl <sub>3</sub> ) spectrum of 9.....	7
Figure S7. <sup>1</sup> H NMR (500 MHz, CDCl <sub>3</sub> ) spectrum of 10.....	Error! Bookmark not defined.
Figure S8. <sup>13</sup> C NMR (126 MHz, CDCl <sub>3</sub> ) spectrum of 10.....	Error! Bookmark not defined.
Figure S9. <sup>1</sup> H NMR (500 MHz, CDCl <sub>3</sub> ) spectrum of D1.....	8
Figure S10. <sup>13</sup> C NMR (126 MHz, CDCl <sub>3</sub> ) spectrum of D1.....	9
Figure S11. <sup>1</sup> H NMR (600 MHz, DMSO- <i>d</i> <sub>6</sub> ) spectrum of D2.....	9
Figure S12. <sup>13</sup> C NMR (151 MHz, DMSO- <i>d</i> <sub>6</sub> ) spectrum of D2.....	10
Figure S13. <sup>1</sup> H NMR (600 MHz, DMSO- <i>d</i> <sub>6</sub> ) spectrum of D3.....	10
Figure S14. <sup>13</sup> C NMR (151 MHz, CDCl <sub>3</sub> ) spectrum of D3.....	11

<b>Figure S15.</b> FTIR spectra of dye powder and dye adsorbed on TiO <sub>2</sub> nanoparticles for <b>D2</b> .....	11
<b>Figure S16.</b> FTIR spectra of dye powder and dye adsorbed on TiO <sub>2</sub> nanoparticles for <b>D3</b> .....	12
<b>Figure S17.</b> Photos of the device <b>D1</b> fixed in the measuring stand.....	12

## General Information

All reagents were purchased from commercial sources and were used without further purification. Compounds **1-4** and **12-14** were synthesized as described by us previously [10]. 1,4-Dioxane for the microwave-assisted Suzuki cross-coupling reaction was deoxygenated by bubbling argon for 1 h.

The <sup>1</sup>H and <sup>13</sup>C NMR spectra were recorded on a Bruker DRX-AVANCE-500 and AVANCE-600 instruments using Me<sub>4</sub>Si as an internal standard. Elemental analysis was carried on a Eurovector EA 3000 automated analyzer. High resolution mass spectrometry was performed using a Bruker maXis Impact HD spectrometer. Melting points were determined on Boetius combined heating stages and were not corrected.

Flash-column chromatography was carried out using Alfa Aesar silica gel 0.040-0.063 mm (230-400 mesh), eluting with chloroform. The progress of reactions and the purity of compounds were checked by TLC on Sorbfil plates (Russia), in which the spots were visualized with UV light (254 or 365 nm).

Microwave experiments were carried out in a Discover SP unimodal microwave system (CEM, USA) with a working frequency of 2.45 GHz and the power of microwave radiation ranged from 0 to 300W. The reactions were carried out in a 35 mL reaction tube with the hermetic silicone cork. The temperature of the reaction was monitored using an inserted IR sensor by the external surface of the reaction vessel.

Thermogravimetric analysis (TGA) was performed using a NETZSCH TG 209 F1 Iris in a temperature range 35-520°C. A sample in an Al<sub>2</sub>O<sub>3</sub> crucible was heated with a constant heating rate, 10 K/min, in a dynamic atmosphere of air (gas flow 30 mL/min). The argon flow (20 ML/min) was used to protect the functional elements of the TGA. The evolved gas was analyzed by QMS 403C Aëolos mass-spectrometric unit coupled with the thermobalances. The ionization electron energy was 70 eV; the ion currents were registered for mass numbers (the mass-to-charge ratio) in the range from 1 to 299 a.m.u.

Absorption spectra of solutions of compounds were recorded (1.0-3.0)×10<sup>-5</sup> M on a Shimadzu UV-2401PC dual-beam spectrophotometer and Cary 5000 UV-Vis-NIR spectrophotometer. Fluorescence spectra of solutions were recorded on a Varian Cary Eclipse fluorescence spectrophotometer. IR spectra of the dye powders and dyes adsorbed on TiO<sub>2</sub> nanoparticles were recorded on a Spectrum One Fourier transform IR spectrometer (Perkin Elmer) equipped with a diffuse reflectance attachment (DRA) in the frequency range 3600±1200 cm<sup>-1</sup>. Spectrum processing and band intensity determination were carried out using the special software supplied with the spectrometer. All measurements were performed at room temperature (20 ± 2 °C).

Electrochemical studies of synthesized molecules were carried out using the PAR (Princeton Applied Research) 273 potentiostat/galvanostat. The standard three-electrode cell equipped with a SU-2000 glassy carbon disc (0.0078 cm<sup>2</sup>) pressed into Teflon as a working electrode, Ag quasi-reference electrode, and a platinum grid (1 cm<sup>2</sup>) as a counter electrode was employed. The cyclic voltammograms (CV) were registered in anhydrous CH<sub>2</sub>Cl<sub>2</sub>

with  $1\text{-}2\cdot 10^{-3}$  M of analyzed compound and 0.1M tetrabutylammonium hexafluorophosphate as supporting electrolyte under high purity argon atmosphere at a scan rate in the range from 0.05 to 1.0 V/s. To HOMO-LUMO energies calculation, the potential of the reference electrode was calibrated by using the ferrocene/ferrocenium (Fc/Fc<sup>+</sup>) redox couple  $E_{1/2}(\text{Fc}/\text{Fc}^+)$  (that was estimated by the CV data as 0.2 V), which has a known oxidation potential of +4.8 eV.

The HOMO and LUMO energy values were estimated from the onset potentials of the first independent oxidation and reduction process, respectively, according to the following equations:

$$E_{\text{HOMO}} (\text{eV}) = - [E_{\text{ox}}^{\text{onset}} - E_{1/2}(\text{Fc}/\text{Fc}^+) + 4.8]$$

$$E_{\text{LUMO}} (\text{eV}) = - [E_{\text{red}}^{\text{onset}} - E_{1/2}(\text{Fc}/\text{Fc}^+) + 4.8],$$

where  $E_{1/2}(\text{Fc}/\text{Fc}^+)$  is the half-wave potential of the Fc/Fc<sup>+</sup> couple (in this work experimentally estimated as 0.2 V) against the Ag electrode.

#### **Fabrication and $J$ - $V$ characterization of DSSCs.**

Three DSSC with different dyes were fabricated using a Solaronix test cell kit. TiO<sub>2</sub> electrodes were immersed in 0.5 mM THF solution of **D1-D3** dyes for 24 h in the dark then washed by 2-propanol to remove the unabsorbed dye and dried at 50 °C for 10 min. After connecting two electrodes by polymer film in a thermal press (Carver) at 100 °C for 3 min, the electrolyte solution in 3-propyl-1-methylimidazolium iodide (PMII, 0.6 M), lithium iodide (LiI, 0.1 M), iodine (I<sub>2</sub>, 0.05 M), and *tert*-butylpyridine (TBP, 0.5 M) in 3-methoxypropionitrile was injected into space between two electrodes and injection hole was sealed. Photoanode active area of all investigated DSSCs was  $6 \times 6 \text{ mm}^2$  (0.36 cm<sup>2</sup>). Additionally, we used a black mask during the electrical measurements for the accurate performance assessment. The current density-voltage ( $J$ - $V$ ) characteristics of fabricated solar cells were determined under irradiation (100 mW/cm<sup>2</sup>) using a Newport 67005 Arc lamp light source with a Xe lamp. The  $J$ - $V$  characteristics were measured using a Keithley 2450 source meter by applying voltage and measuring current.

#### **Characterization of photoanodes by modulation spectroscopy.**

Photoanodes were prepared in the following manner. TCO22-15 glass (2.9×2.9 cm<sup>2</sup> pieces) coated with a conductive indium tin oxide (specific surface resistivity about 15 Ω/sq, Solaronix) was purified by ultrasonication in organic solvents (isopropanol and acetone) and distilled water, and then dried at 50 °C in air. Application of Tinanoxide D/SP paste (Solaronix), comprising a nanocrystalline TiO<sub>2</sub>, was performed by the standard "doctor blade" procedure, using a stencil with a square hole of  $6 \times 6 \text{ mm}^2$  and a depth of ~90 μm. After application of the paste, raw photoanodes were dried at 50 °C in air, and then calcined in a muffle furnace at 450 °C for 1 h with heating rate of 3 °C/min. The heat treatments were carried out in the air. The thickness of thus obtained TiO<sub>2</sub> film was about 15 nm. Sensitizing of titanium dioxide was performed by soaking photoanodes in 0.5 mM THF solution of dye (**D1** and **D3**) for 24 h in the dark.

The photoelectrochemical characteristics of photoanodes were studied using a three-electrode PECC-2 cell (Zahner Elektrik). The photoanode served as the working electrode. A platinum wire (5 cm<sup>2</sup>) and a silver wire were used as the auxiliary and quasi-reference electrodes. As electrolyte used acetonitrile solution of 0.5 M LiI + 0.05 M I<sub>2</sub>. The voltammetric measurements were performed with an IPC Pro MF potentiostat. The working electrode was

illuminated with a Newport 96000 AM 1.5 solar spectrum simulator with power of 100 mW/cm<sup>2</sup>. The illumination power at different distances was controlled with a Nova apparatus (OPHIR-SPIRICON Inc.). The time dependence of the photoanode potentials under the open-circuit conditions and the photocurrents at the short-circuit potential (transients) were measured under both illumination and in dark.

The recombination characteristics were studied using the methods of intensity modulated photocurrent spectroscopy (IMPS) and intensity modulated photovoltage spectroscopy (IMVS) [11,12]. IMPS and IMPS measurements were conducted on a ZAHNER's CIMPS-QE/IPCE workstation. The working electrode was illuminated with a tunable light-source, TLS03. IMVS were taken without superposition of external polarization, i.e., under open circuit (OC) conditions. IMPS were recorded under short-circuit (SC) conditions.

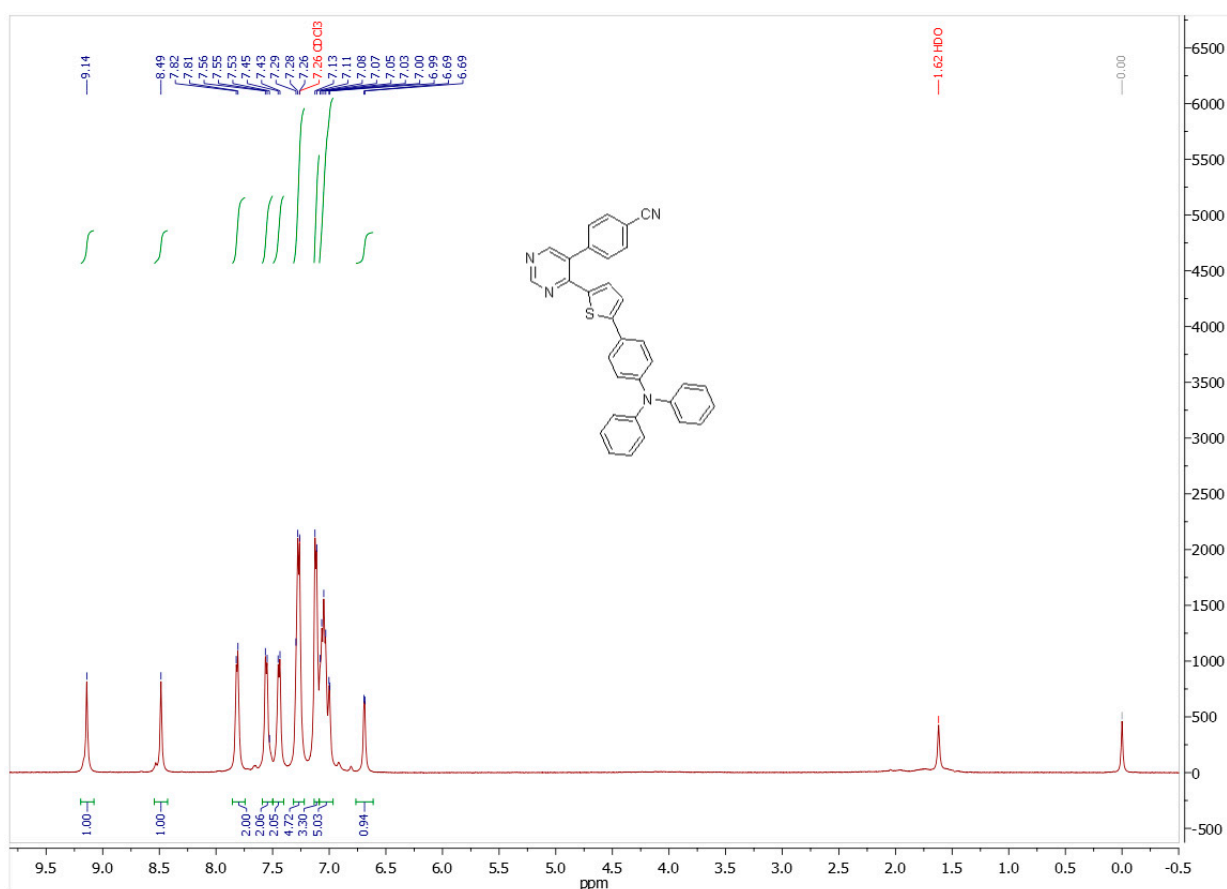


Figure S1. <sup>1</sup>H NMR (500 MHz, CDCl<sub>3</sub>) spectrum of 6.

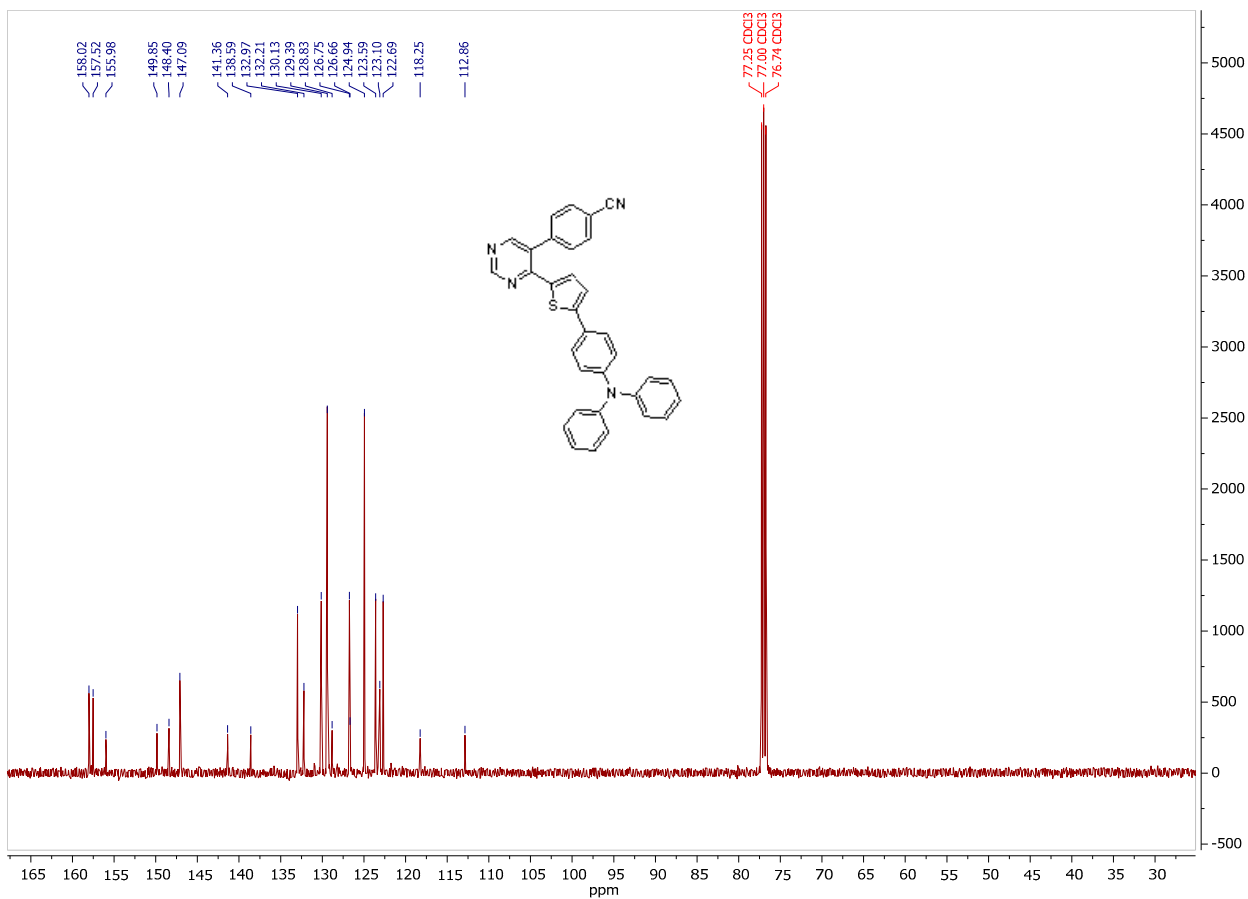


Figure S2. <sup>13</sup>C NMR (126 MHz, CDCl<sub>3</sub>) spectrum of 6.

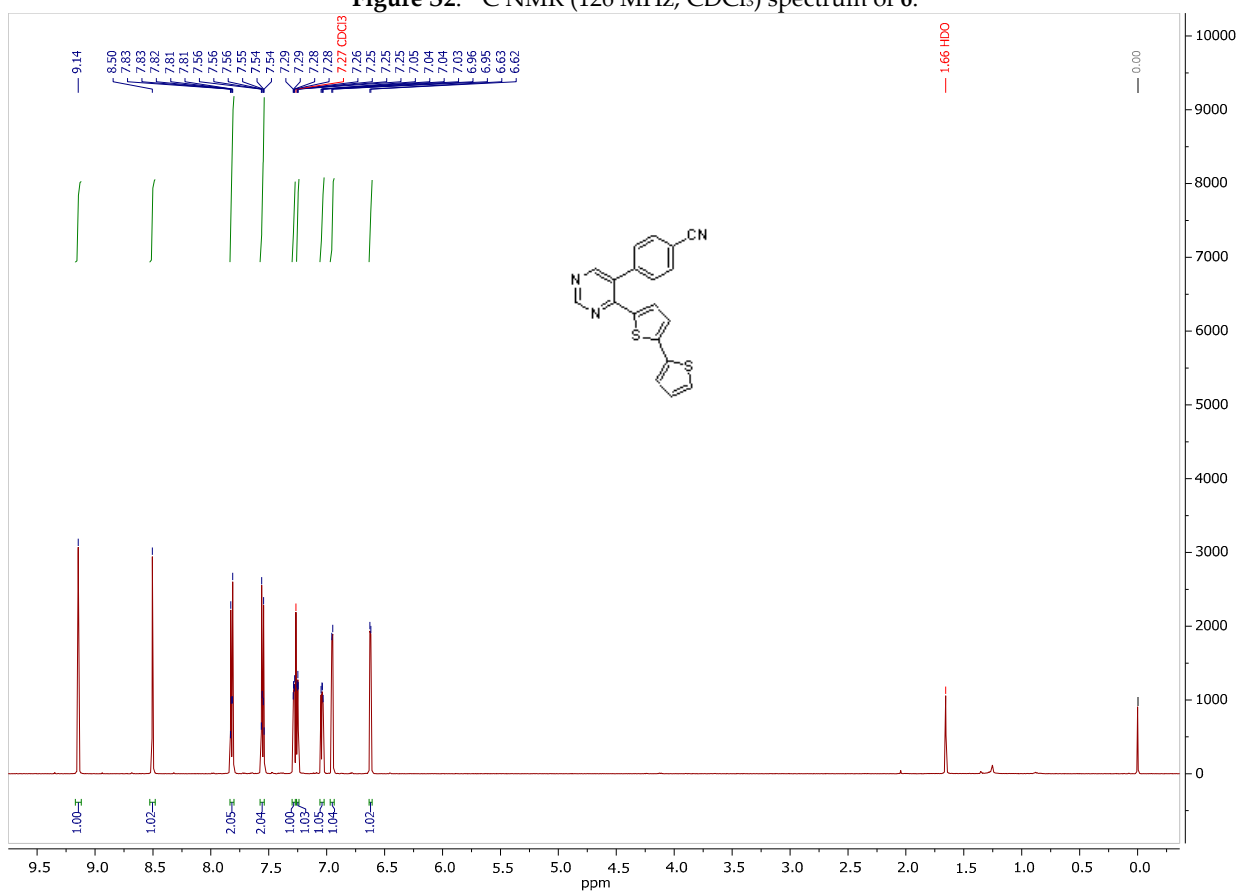


Figure S3. <sup>1</sup>H NMR (500 MHz, CDCl<sub>3</sub>) spectrum of 8.

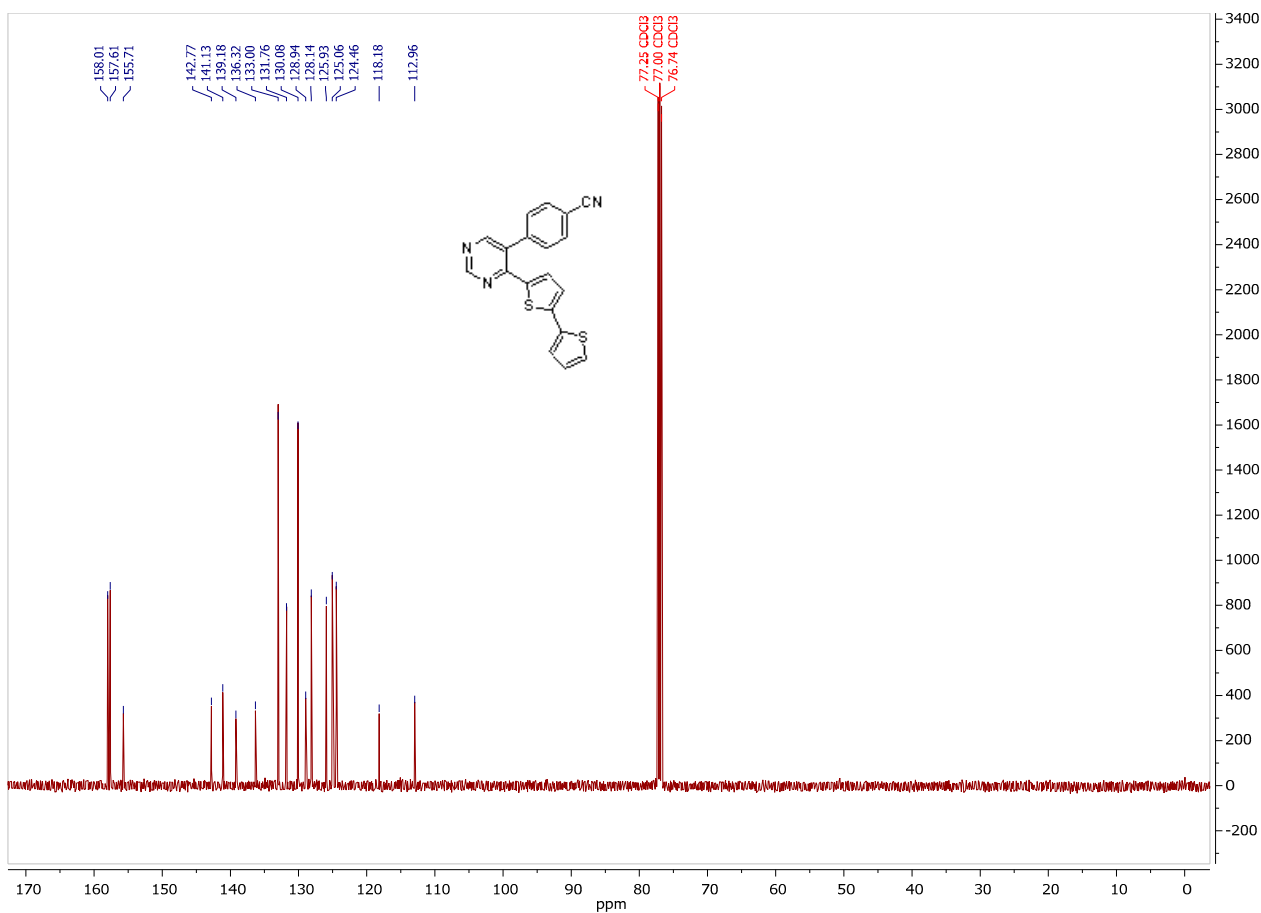


Figure S4.  $^{13}\text{C}$  NMR (126 MHz,  $\text{CDCl}_3$ ) spectrum of 8.

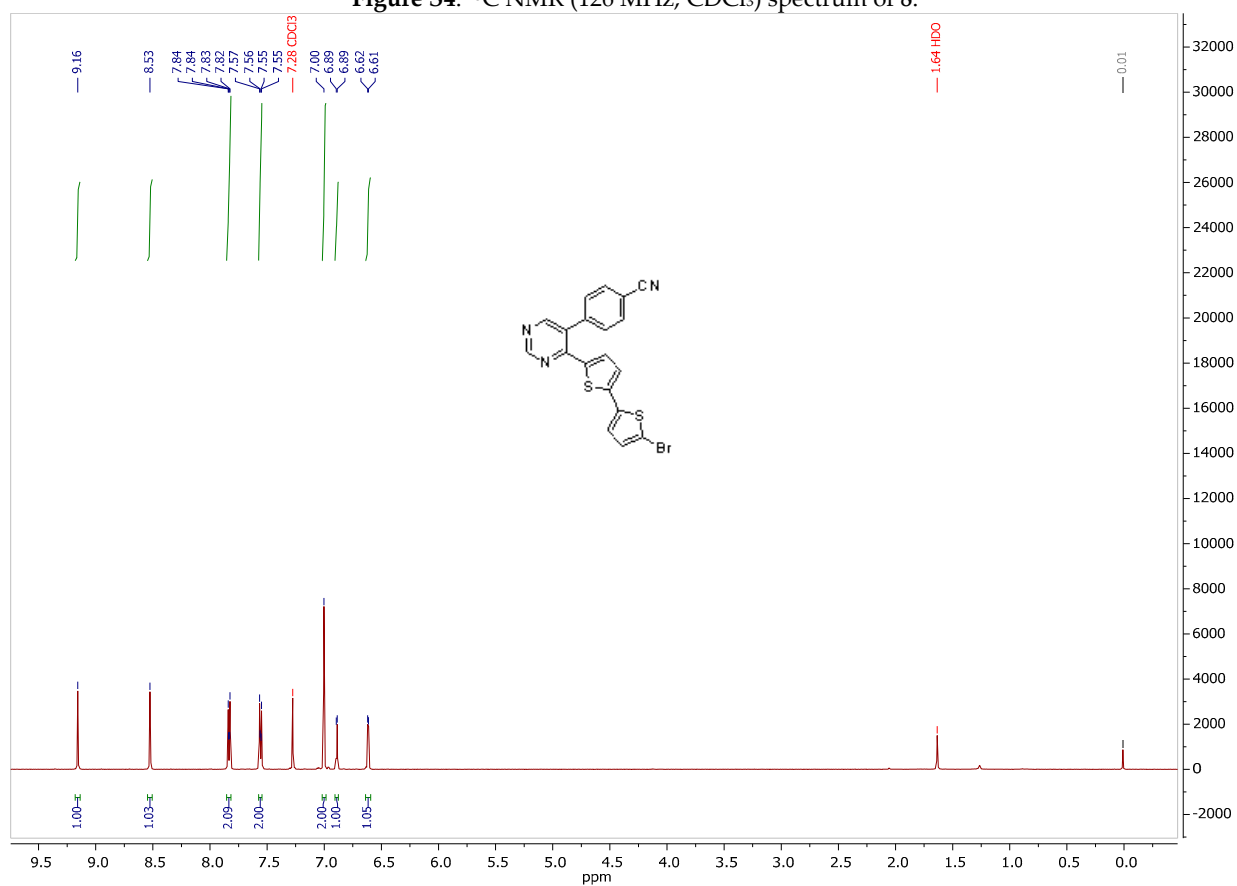


Figure S5.  $^1\text{H}$  NMR (500 MHz,  $\text{CDCl}_3$ ) spectrum of 9.

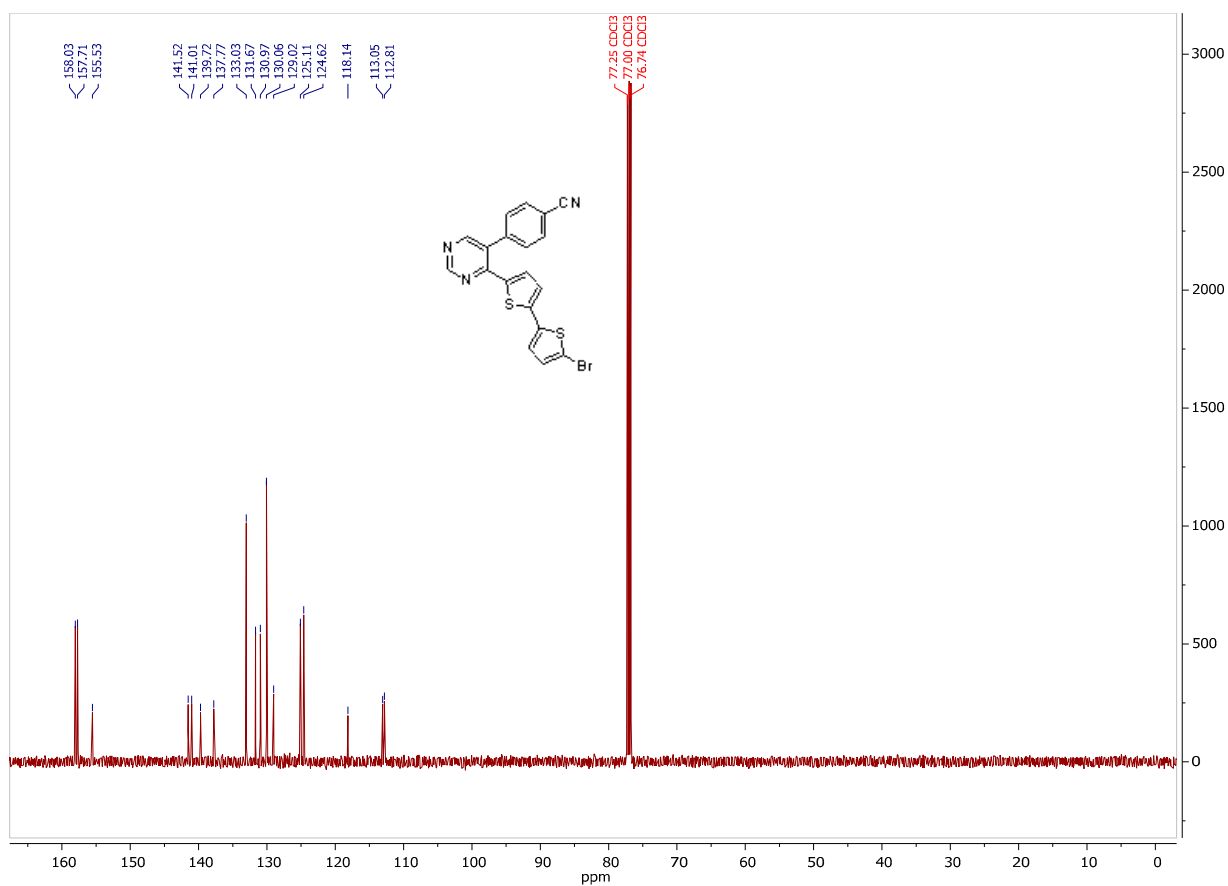


Figure S6.  $^{13}\text{C}$  NMR (126 MHz,  $\text{CDCl}_3$ ) spectrum of 9.

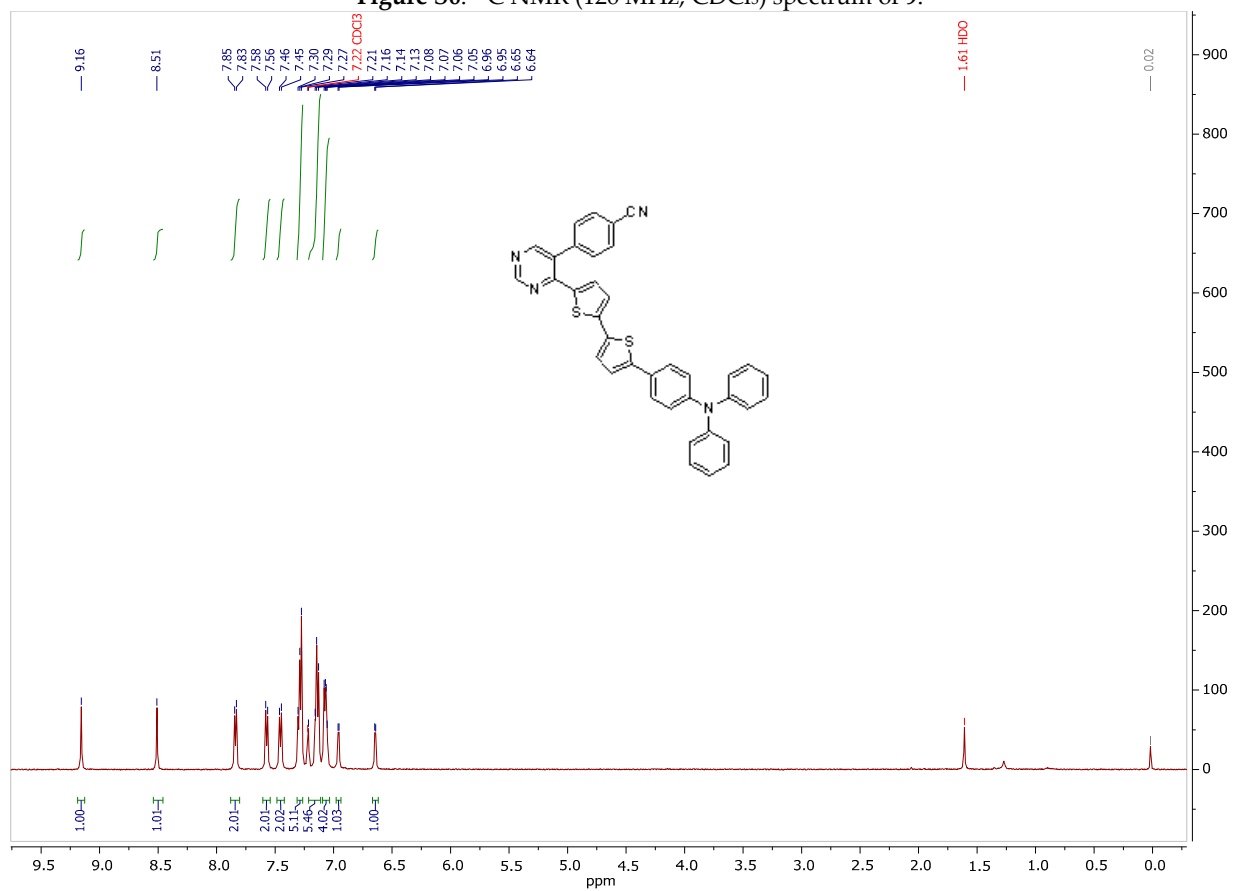


Figure S7.  $^1\text{H}$  NMR (500 MHz,  $\text{CDCl}_3$ ) spectrum of 10.

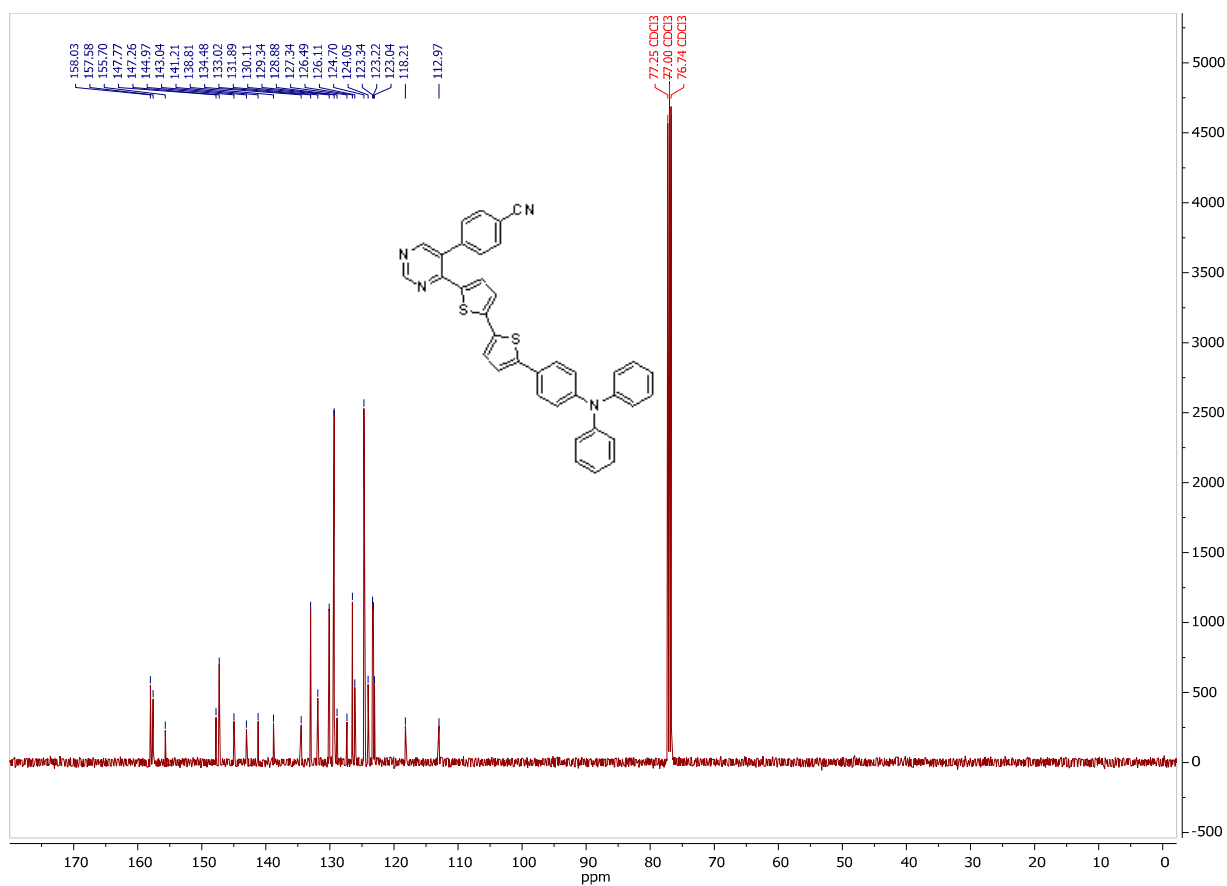


Figure S8. <sup>13</sup>C NMR (126 MHz, CDCl<sub>3</sub>) spectrum of 10.

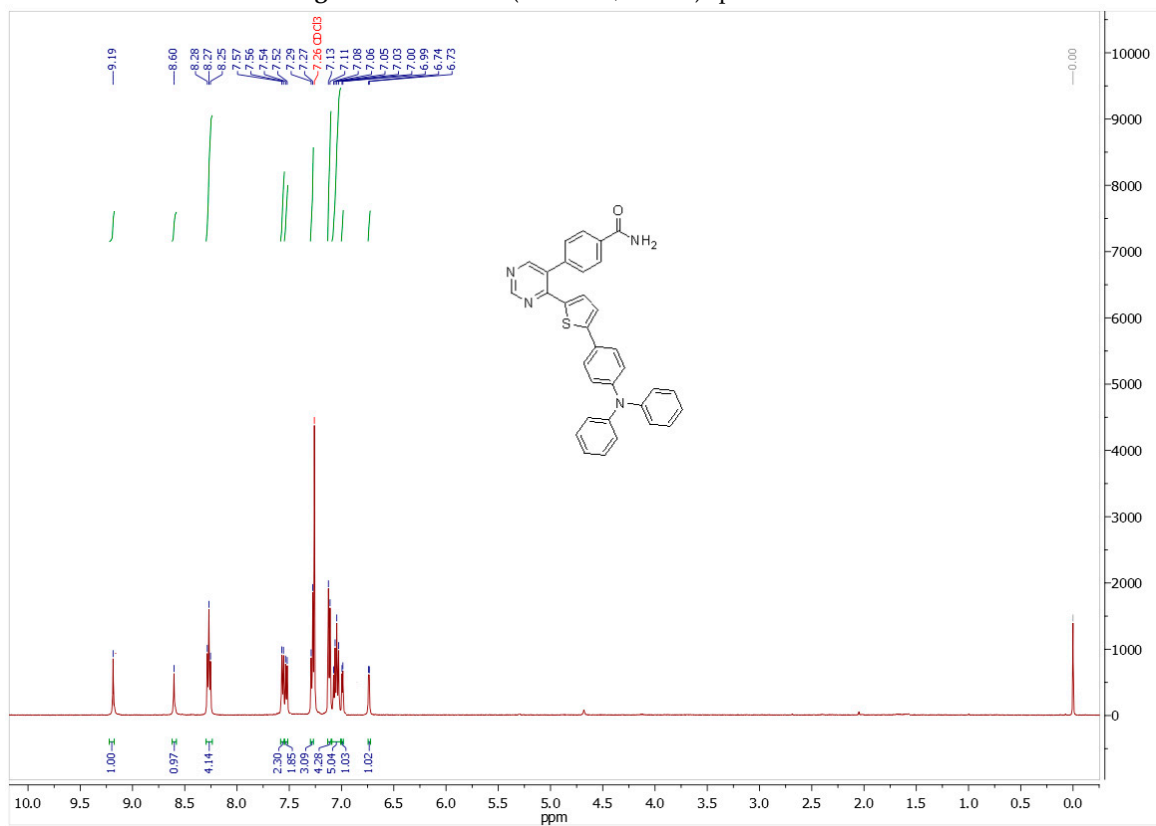


Figure S9. <sup>1</sup>H NMR (500 MHz, CDCl<sub>3</sub>) spectrum of D1.

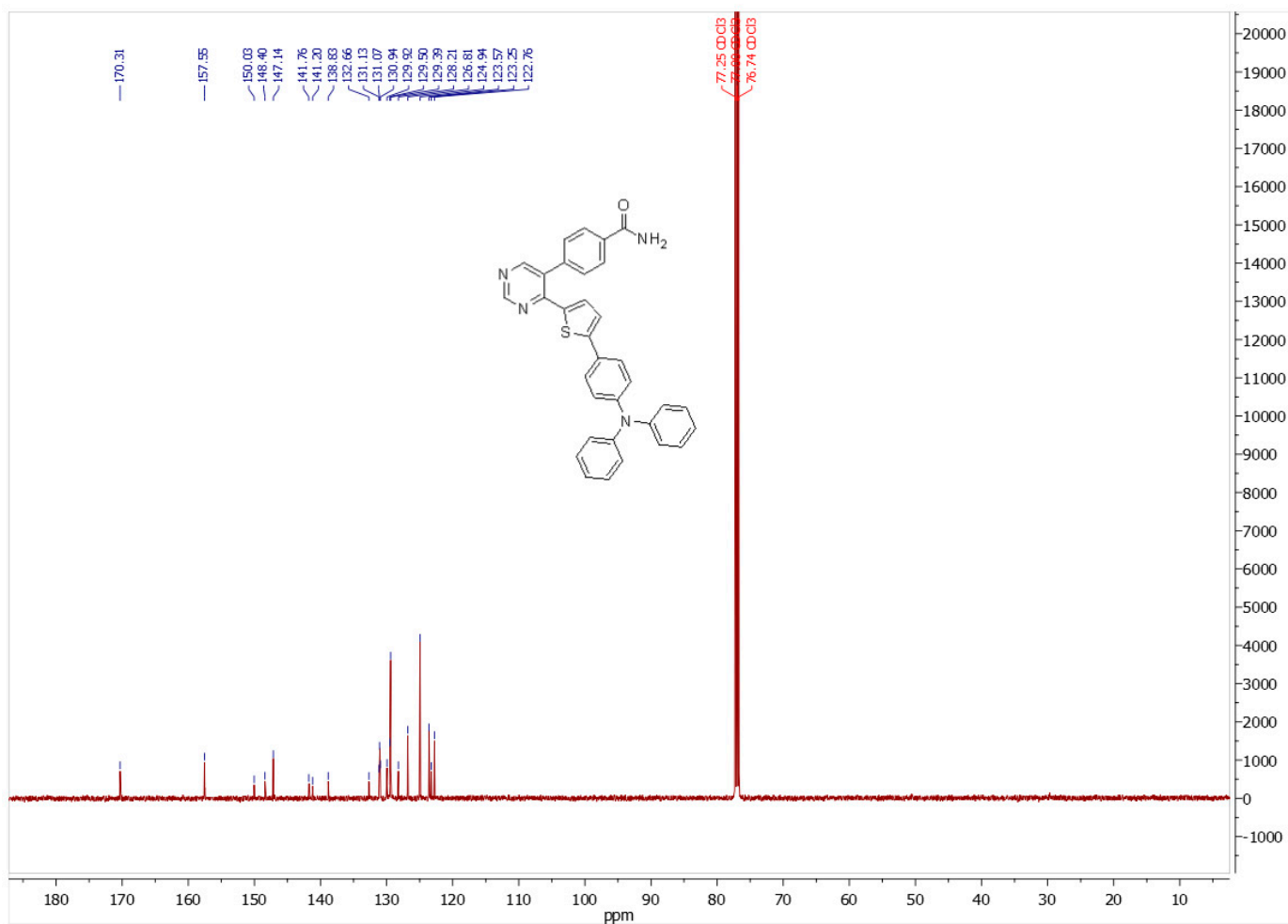


Figure S10. <sup>13</sup>C NMR (126 MHz, CDCl<sub>3</sub>) spectrum of D1.

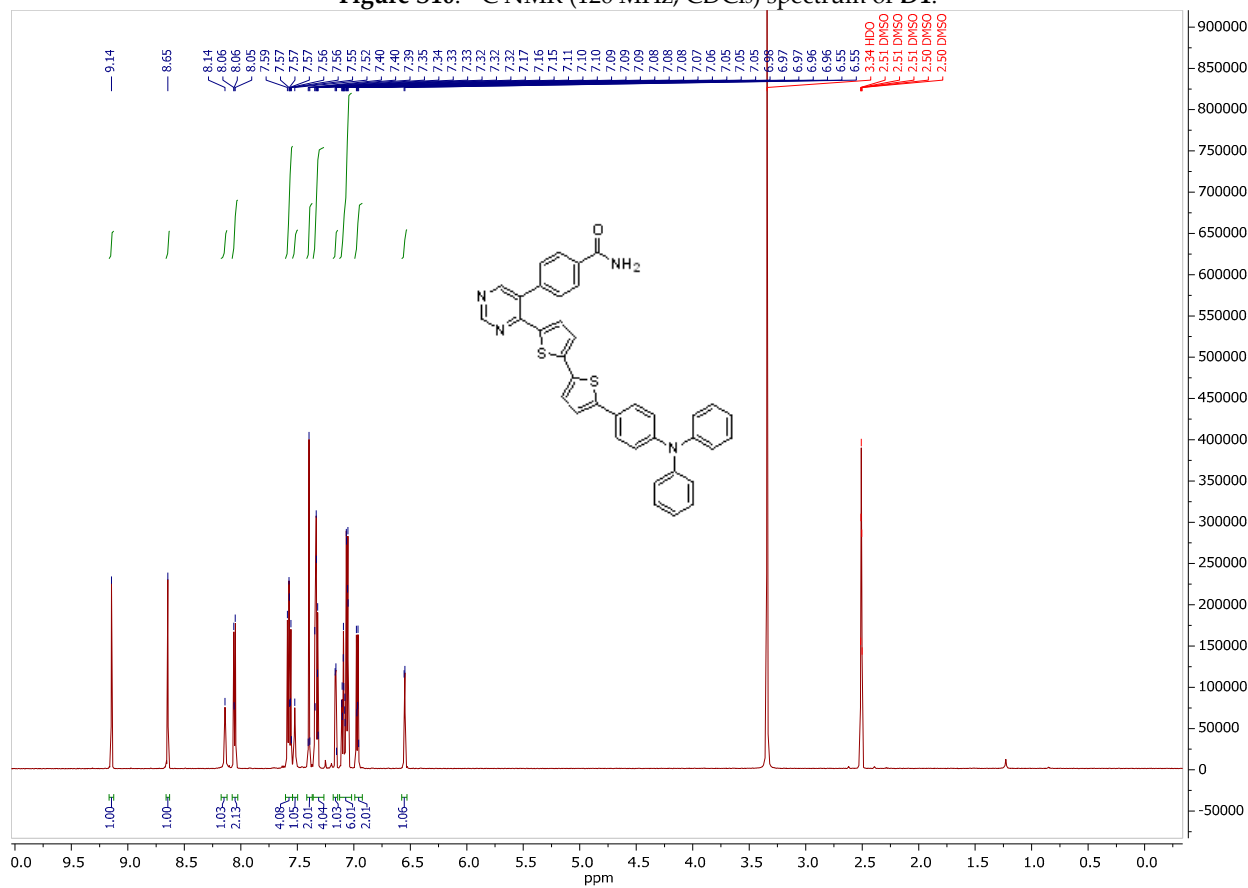


Figure S11. <sup>1</sup>H NMR (600 MHz, DMSO-*d*<sub>6</sub>) spectrum of D2.

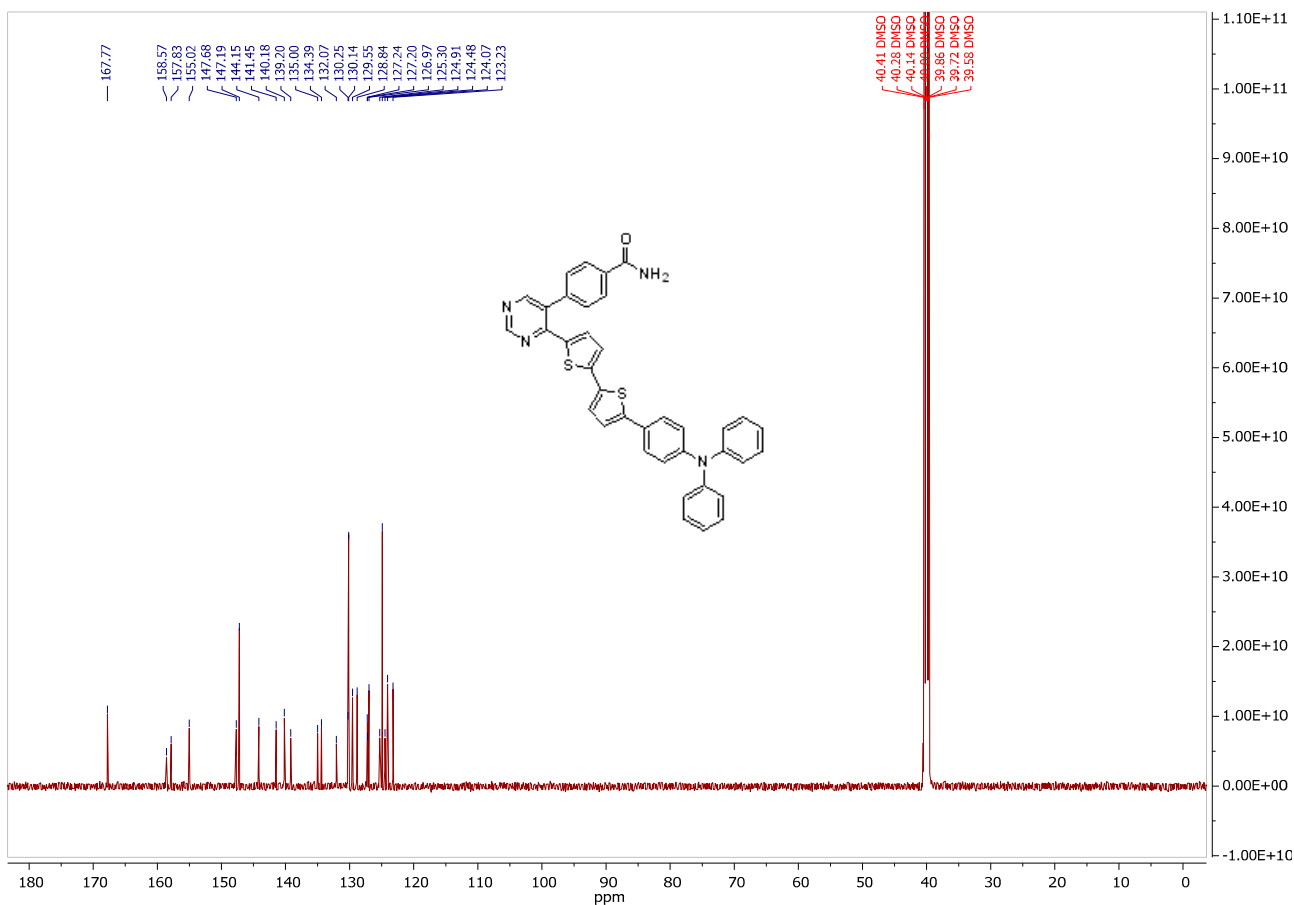


Figure S12. <sup>13</sup>C NMR (151 MHz, DMSO-*d*<sub>6</sub>) spectrum of D2.

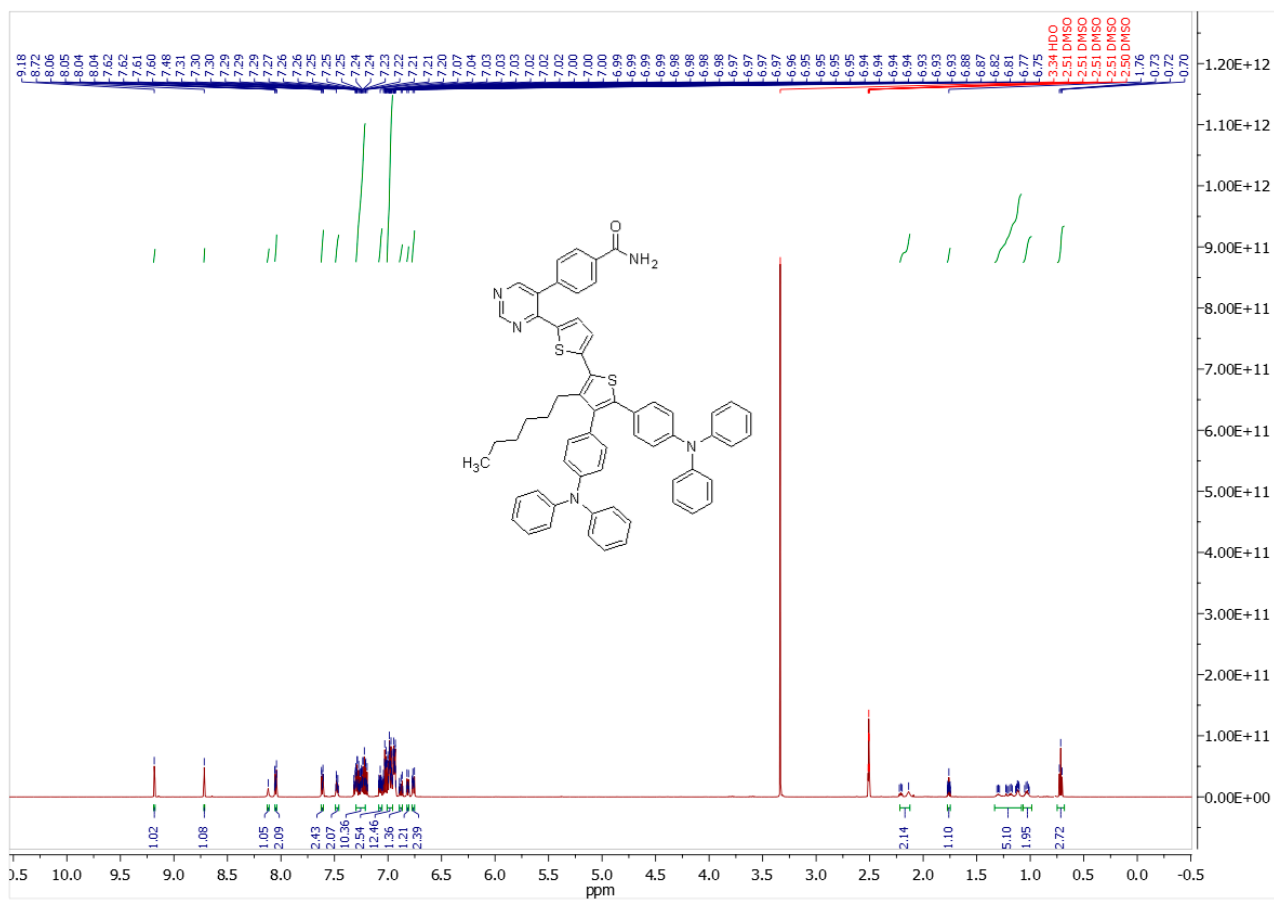


Figure S13. <sup>1</sup>H NMR (600 MHz, DMSO-*d*<sub>6</sub>) spectrum of D3.

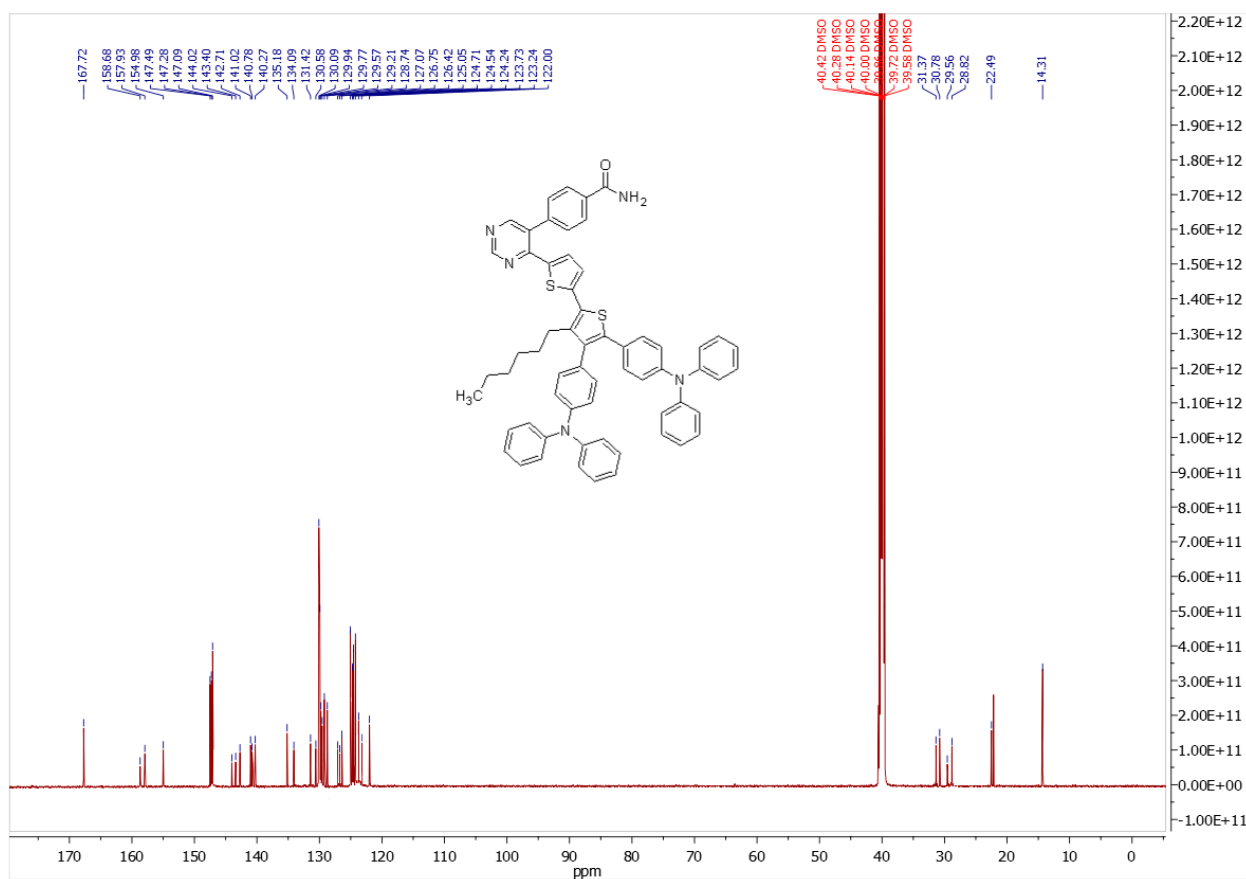


Figure S14.  $^{13}\text{C}$  NMR (151 MHz,  $\text{CDCl}_3$ ) spectrum of D3.

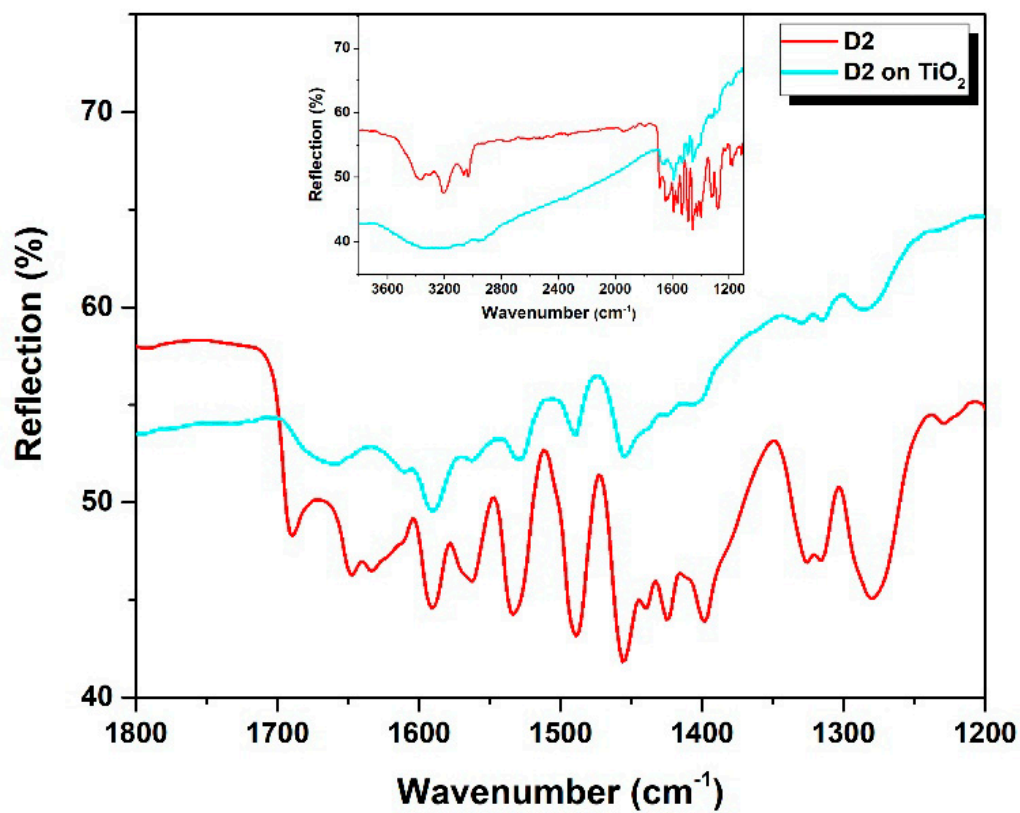


Figure S15. FTIR spectra of dye powder and dye adsorbed on  $\text{TiO}_2$  nanoparticles for D2.

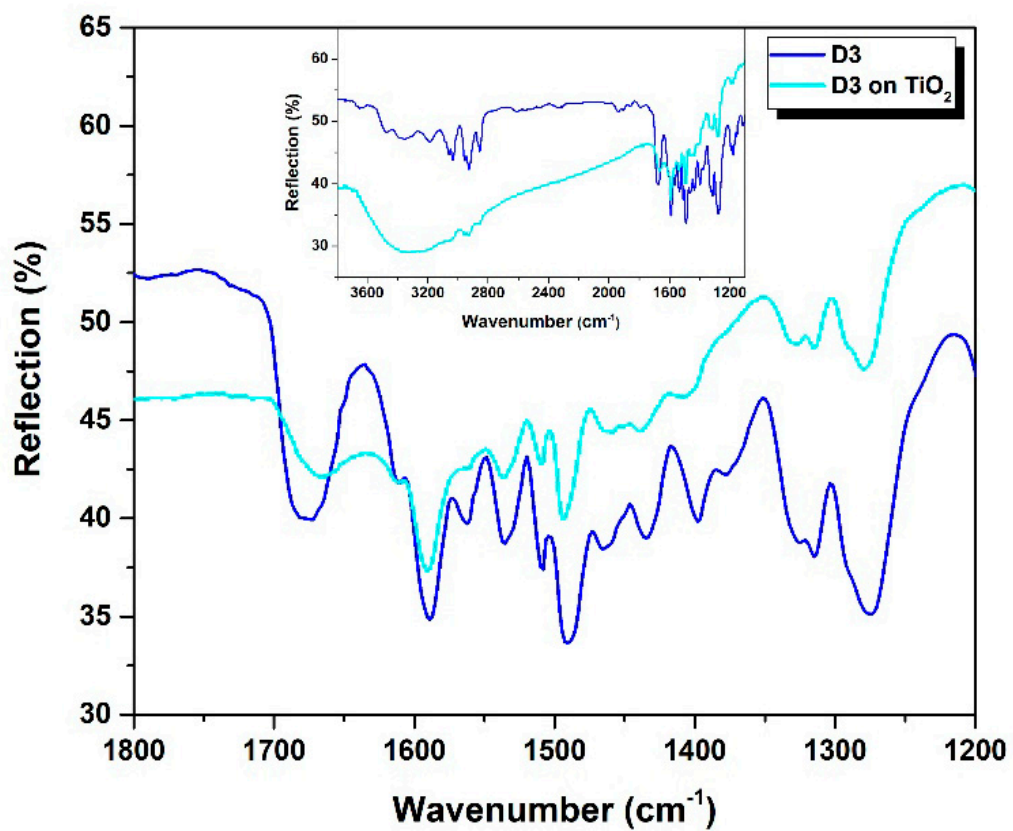


Figure S16. FTIR spectra of dye powder and dye adsorbed on TiO<sub>2</sub> nanoparticles for D3.

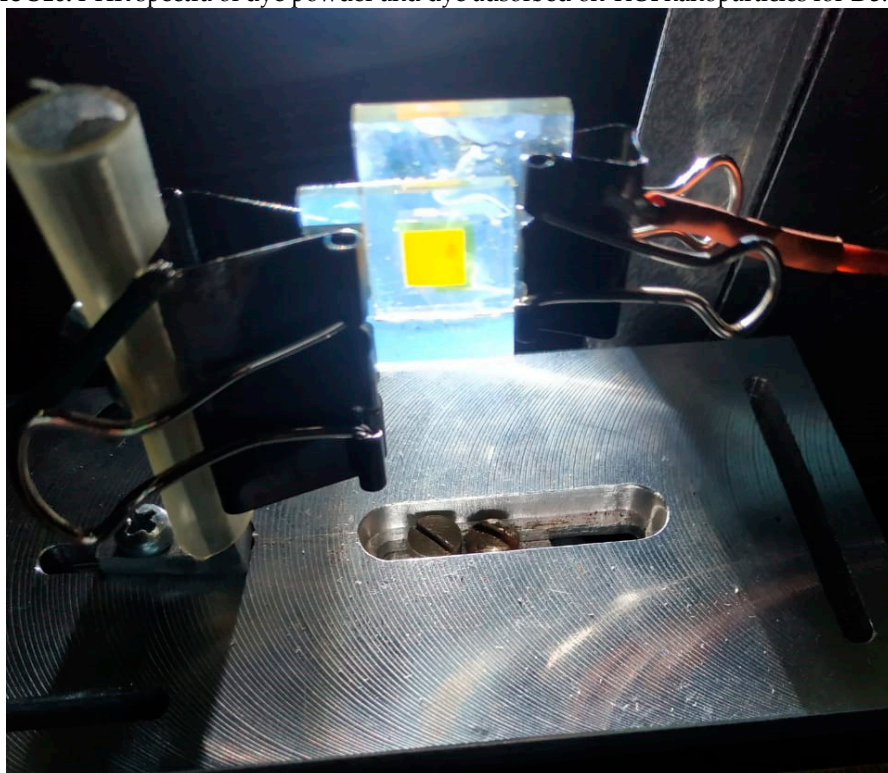


Figure S17. Photo of the device D1 attached to the measurement stand.